International Symposium on Solar Physics and Solar Eclipses (SPSE) 2006
R. Ramelli, O. M. Shalabiea, I. Saleh, and J.O. Stenflo, eds.

MEASUREMENTS OF ATOMIC AND MOLECULAR PARAMETERS OF HYDROGEN AND NITROGEN FOR SOLAR PHYSICS

ADRIAN DAW*, ANTHONY G. CALAMAI*, SAMUEL BREWER† and BRIAN MYER‡
Department of Physics and Astronomy, Appalachian State University, Boone, NC 28608, USA

and

DANIEL WOLF SAVIN and MICHAEL SCHNELL
Columbia Astrophysics Laboratory, Columbia University, New York, NY 10027, USA

Abstract. Experiments in progress at Appalachian State University's Ion Trap Laboratory are providing atomic and molecular data for solar, stellar, planetary, and astrophysical plasmas: collision rates coefficients, radiative decay rates of metastable ions, and unimolecular dissociation rates of ionized molecules. Processes currently under study include: collision rates of protons with H_2 and He, of atomic and molecular nitrogen ions with N_2, radiative decay of metastable $2s2p^3\ {}^5S_2$ N^+, and the dissociation rate of doubly-ionized molecular nitrogen. The first results of these investigations are presented, and the radio-frequency ion trap apparatus and its many capabilities to provide data for solar physics and related fields are discussed.

Key words: atomic and molecular data, ultraviolet spectroscopy, solar activity, sunspots, aurora, protons, hydrogen, nitrogen

1. Introduction

Understanding the macroscopic behavior of solar and stellar plasmas, and obtaining physical information from analysis of spectra of these plasmas, requires reliable, quantitative information on the fundamental atomic and molecular parameters of the constituent ionic and neutral species. The Ion Trap Laboratory at Appalachian State University has the ability to provide such information, that is, to measure: ion-neutral reaction rate coefficients for processes such as electron capture and proton capture, branching fractions into different excited states for such reactions, collisional de/excitation rate coefficients, unimolecular dissociation rates for ionized molecules, and radiative decay rates of metastable ions.

Currently, we are measuring: (*i*) rate coefficients for proton collisions with H_2 and He, which are important to the coupling of proton and neutral flows in sunspots, and (*ii*) the following parameters of nitrogen important throughout the heliosphere: the radiative lifetime of the ${}^5S_2$ metastable level of N^+, the dissociation rate of N_2^{++}, electron capture rate coefficients by N^+ and N_2^{++} from molecular nitrogen, and the

* dawan@appstate.edu, calamaiag@appstate.edu, http://www.phys.appstate.edu
† Chemical Physics Program, University of Maryland, College Park, MD 85721, USA
‡ College of Optical Sciences, University of Arizona, Tucson, AZ 20742, USA

cross section for dissociative electron impact ionization of molecular nitrogen into metastable $^5S_2$ N^+.

Just as atomic physics, plasma physics, and solar physics are intrinsically connected, solar activity and its impact on the heliosphere are intrinsically connected to the study of planetary atmospheres, particularly ionospheres. Radiative decay of metastable $^5S_2$ N^+ results in an emission line doublet at 213.90 and 214.28 nm, an important feature in UV spectra of the Earth's ionosphere which has been referred to as the 'auroral mystery feature', owing to the controversy surrounding its identification and the uncertainties in the atomic parameters (Dalgarno *et al.*, 1981, Bucsela & Sharp, 1989, Meier, 1991, Bucsela *et al.*, 1998). Although the N II] doublet has received considerable attention and some issues have been resolved, there are a number of important issues remaining which will be addressed by this work, as discussed in section 2.1.

Mendoza, Zeippen and Storey (1999) performed a detailed theoretical study of the radiative decay properties of the $^5S_2$ metastable state in the carbon isoelectronic sequence, and concluded, "we would welcome further theoretical and experimental benchmarks that would clarify the inconclusive situation regarding the lifetimes and branching ratios" for the low-charge-state end of this sequence. Our measurement of the radiative decay rate of $^5S_2$ N^+ will thus also help clarify the radiative decay of $^5S_2$ O^{++}, which gives rise to the O III] doublet at 166.08 and 166.61 nm in solar spectra. The intensity of O III] is very sensitive to small variations in electron density, which makes it an important spectroscopic diagnostic of chromosphere-corona transition regions (Del Zanna *et al.*, 2002, Mason & Monsignori Fossi, 1994, Bhatia *et al.*, 1982). The intensity of N II] could also potentially be used as a diagnostic for solar plasmas, but few observations of solar spectra cover the wavelength 214 nm. Vernazza and Reeves (1978), for example, observed the radiative decay of the $^5S_2$ metastable level in carbon-like Ca, Ar, S, Si, Al, Mg, Na, Ne, and F, but O III] and N II] were outside the wavelength range of the observations (28 to 135 nm). Nevertheless, excitation out of $^5S_2$ N^+ gives rise to emission lines such as those at 50.6 and 62.9 nm, which can also be used as a diagnostic. For such diagnostics that involve excitation out of the metastable level, it is the total radiative decay rate, hence the lifetime, for the metastable level's downward transitions that are critical, not the radiative decay rate of the transition observed (*e.g.*, Mason & Monsignori Fossi, 1994). The other critical parameters for such diagnostics are the electron impact de/excitation rate coefficients, which have recently been calculated by Hudson & Bell (2005).

First results for the radiative lifetime of $^5S_2$ N^+ are presented in section 2, as are first results for the dissociation rate of N_2^{++}. Other parameters to be measured are collisional rate coefficients, and the cross section for dissociative electron impact ionization of molecular nitrogen into metastable $^5S_2$ N^+, which is responsible for auroral 214 nm emission. As discussed in section 2.1, estimates for this cross section span a factor of 4. The measurement of this cross section will help resolve whether the primary excitation mechanism for ionospheric N II] is solar photons or auroral electrons (Victor & Dalgarno, 1982, Siskind & Barth, 1987, Cleary & Barth, 1987, Meier, 1991).

To measure atomic and molecular parameters, ions are created in a radiofrequency (RF) ion trap during a 'fill' period by electron impact ionization of gas admitted into a vacuum chamber. Following the fill period, the number of ions stored is measured as a function of time, and for the nitrogen parameters, the number of UV photons emitted in different bandpasses by radiative decay of metastable states and excited reaction products is also measured as a function of time. A detailed consideration of all collisional and non-collisional rates yields a function, typically an exponential decay, which is fit to the data to determine fundamental atomic and molecular parameters. The nitrogen measurements are discussed in section 2.

The proton-hydrogen and proton-helium measurements, which pertain to the coupling of ion and neutral flows in sunspots and to star formation in the early universe, are discussed in section 3.

The apparatus and method are explained in the context of these measurements, and readers are encouraged to consider parameters required for their research that could be measured using this apparatus. A brief final discussion is given in section 4.

2. Nitrogen Measurements

The nitrogen parameters being measured are:

- The radiative lifetime of the $2s2p^3\ {}^5S_2$ metastable level of N^+
- Rate coefficients for quenching of ${}^5S_2\ N^+$ (and thus N II]) by collisions with N_2
- The cross section for production of ${}^5S_2\ N^+$ by electron impact ionization of N_2
- The unimolecular dissociation rate of the molecular dication N_2^{++}
- Rate coefficients for the electron capture reaction $N_2^{++} + N_2 \rightarrow N_2^+ + N_2^+$
- Branching fractions into different excited states for this reaction

Ions are created in a RF ion trap (see Fig. 1) by electron impact ionization of N_2 gas, and the UV radiation emitted by the stored ion population is then measured as a function of time. The primary source of radiation is the decaying ${}^5S_2$ metastable N^+ ions, which emit photons at a wavelength of 214 nm. In addition to the atomic N^+, doubly-charged molecular ions, or dications, are created and stored, as both ions have the same charge-to-mass ratio. Electron capture by dications from neutral molecules into excited states of singly-charged molecular nitrogen results in emission in bands that overlap with 214 nm (see Fig. 2). The decay rate of these two sources of radiation is measured as a function of nitrogen gas pressure to determine the electron capture rates for both ions, the radiative decay rate of the metastable ${}^5S_2$ N^+, and the dissociation rate of the dications. The photon observations are corrected for ion losses using the technique presented in Daw (2000). The cross section for dissociative electron impact ionization of molecular nitrogen into metastable ${}^5S_2\ N^+$ will be determined relative to the (well-known) cross section for dication production, by comparing the photon rate at 214 nm to the photon rate generated in different bandpasses as a result of dication electron capture, as discussed in section 2.3.

2.1. Motivation

The ${}^5S_2\ N^+$ emission at 214 nm is an important feature in spectra of the Earth's aurora and dayglow that results from dissociative ionization of N_2. Despite the importance of this emission and the attention it has received, interpretation of ionospheric observations is hampered by uncertainties in the atomic and molecular pa-

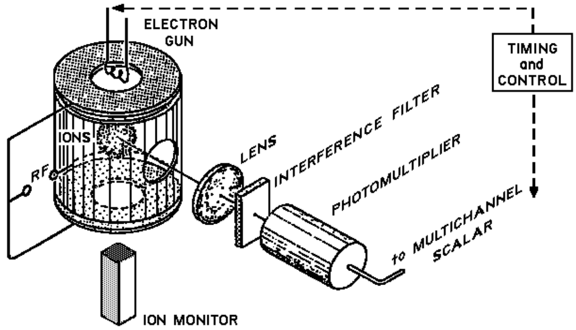

Fig. 1. A diagram showing the ion trap apparatus and elements of the optical detection system.

States of N_2^+ and N^+

Ion	State	r_e(Å)	E (eV above ground)	
N_2^+	$C\,^2\Sigma_u^+$	1.26	7.9	
	$D\,^2\Pi_g$	1.47	6.4	
	$B\,^2\Sigma_u^+$	1.07	3.1	205 to 307 nm
	$A\,^2\Pi_u$	1.17	1.1	138 to 206 nm
	$X^2\Sigma_g^+$	1.12	0	
N^+	$2s2p^3\ ^5S_2$		5.80	
	$2s^22p^2\ ^1S_0$		4.05	
	$2s^22p^2\ ^1D_2$		1.90	214 nm
	$2s^22p^2\ ^3P_{0,1,2}$		0 - 0.016	

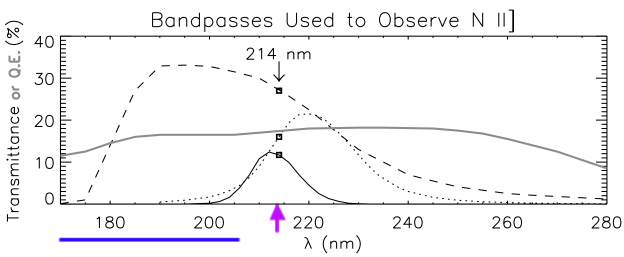

Fig. 2. *Top*: A diagram indicating the observed atomic and molecular transitions on a table of N^+ and N_2^+ states. *Bottom*: A plot of bandpasses used for the observations. The *grey line* is the quantum efficiency of the photomultiplier tube, while the *solid, dotted and dashed lines* are transmittances of different interference filters used for the observations.

rameters. For instance, estimates (mainly deduced from ionospheric observations) of the maximum cross section for electron-impact dissociative ionization into $^5S_2$ N^+ vary between 1×10^{-18} and 4×10^{-18} cm^2 (Dalgarno *et al.*, 1981), and although the energy dependence has been measured (Erdman & Zipf, 1986), knowledge of the absolute value of the cross section has not improved significantly since then. In reference to ionospheric N II] emission, Bucsela *et al.* (1998) urge caution in adopting atomic and molecular constants that are deduced from observations.

Concerning this problem, significant progress has been made in recent years on the radiative lifetime of $^5S_2$ N^+, both theoretically and experimentally, but significant discrepancies still exist between the experimental results (Träbert *et al.*, 1998) and theoretical results (Brage *et al.*, 1997, Mendoza *et al.*, 1999, Tachiev & Froese Fischer, 2001), and further work is needed to resolve this issue. Thus, the lifetime, excitation rate, and quenching rate measurements for $^5S_2$ N^+, from this work will improve our understanding of ionospheres, of the solar photon and particle fluxes that bombard them, and of the underlying atomic physics.

The N_2^{++} dissociation rate, the rate coefficient for $N_2^{++} + N_2 \rightarrow N_2^+ + N_2^+$, and the branching fraction measurements are perhaps most relevant to the ionosphere of Titan (Lilensten *et al.*, 2005). As the importance of their role in the physics and chemistry of plasmas is realized, the structure and reactivity of molecular dications such as N_2^{++} has been the subject of increasing theoretical and experimental attention in recent years, and methods for understanding these challenging systems are developing (Mathur, 2004, Price, 2003, Cox *et al.*, 2003). For Instance, knowledge of the dissociation rate from the lifetime of N_2^{++} in a storage ring (~3 s) represents only an order of magnitude estimate (Mathur, 2004). Mathur also indicates that state-resolved studies of low-energy reactions between dications and neutral molecules will help clarify our understanding of dication systems. Moreover, with a significant abundance of N_2^{++} in some ionospheres, the reaction rate for $N_2^{++} + N_2 \rightarrow N_2^+ + N_2^+$ is important to the chemical pathways of such ionospheres.

2.2. Apparatus

Ions are created during a fill period by biasing the electron gun to ~100 V, and are stored by a combination of RF (~250 V at 1 MHz) and DC potentials on the ring electrode (see Fig. 1). Of the $m/q = 14$ ions created by electron impact on N_2, 11% are N_2^{++}, and the remainder are N^+ (Halas & Adamczyk 1972). Trap cycles comprise a fill period (typically 5 ms) followed by a data collection period. Light emitted as a result of collisions and by decaying metastable ions is focused by a CaF_2 lens onto an EMR 541Q photomultiplier tube (PMT) operated in photon counting mode. Interference filters are used to select different bandpasses. Photon data is accumulated over an even number of trap cycles. On alternate cycles, the trap is emptied, or 'detuned', by raising the upper end cap voltage and lowering the lower end cap voltage, and counts are subtracted from the photon signal to provide subtraction of the ~0.5 count/s PMT dark rate and fluorescence of trap components (see Fig. 3). Every few hours, the photon collection is interrupted to collect ion data. To determine the relative number of ions remaining after a given storage time, a dump pulse is applied to the end caps (typically +60 and -60 V), ejecting the ion cloud through the lower end cap and onto a channel electron multiplier (CEM) operated in analog amplification mode. Further details of ion detection may be found in section 3, and data collected with the apparatus may be seen in Fig. 3.

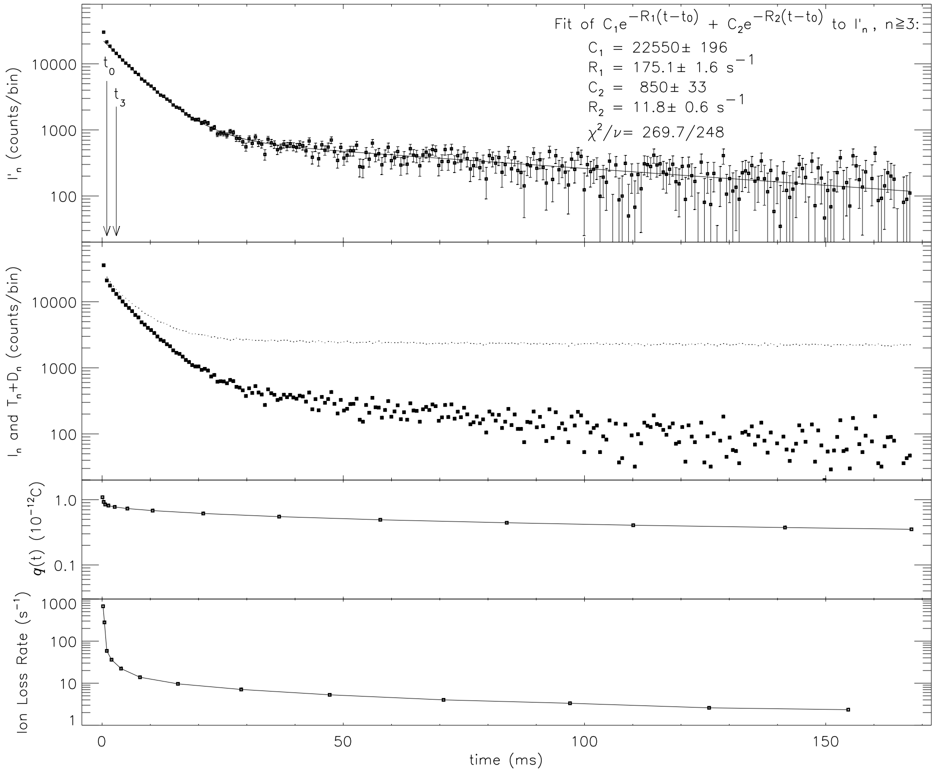

Fig. 3. An example data run comprising 4,781,130 tune/detune cycles of photon collection, taken with N_2 pressure 1.5×10^{-7} torr. *Top*: decay curve obtained by dividing the photon signal by the relative number of ions *vs.* time, as explained briefly here. *Second from top*: For each 0.655 ms bin, the photon signal (*small black squares*) is the number of photons observed during the tuned phase of the cycle minus the number observed during the detune phase: $I_n = T_n - D_n$, where the index indicates bin number. The total $T_n + D_n$ counts per bin are shown by the *tiny dots*, except for the first bin, where $T_n + D_n = 1{,}077{,}357$. Note that n=0 denotes the second bin, as the first bin includes counts from excited neutrals remaining briefly in the field of view after the end of the fill period. *Third from top*: For every photon collection interval (typically 10^5 T/D cycles), the amplified ion cloud charge, $q(t)$, was measured for a number of values of t. The *small black squares* show the average of the data taken for all photon collection intervals. The relative number of ions for each bin is determined by interpolating between the $q(t)$ measurements and is given by $Q(t_n) = q(t_n)/q(t_0)$, so that $I'_0 = I_0$. *Bottom*: Ion loss rate shown for discussion. *Back to the Top*: so explicitly, each point in the decay curve is given by $I'_n = I_n/Q(t_n)$ and has an uncertainty $\sigma_n = \sqrt{T_n + D_n}/Q(t_n)$. Equation 6, specifically, $I'(t - t_0)$, was fit to the data skipping the first 2.62 ms to allow the ion detection system to recover from the fill period, with the results shown above.

2.3. Data and Analysis

The method used for these measurements includes a number of extensions of the method developed to measure the radiative lifetime of the $^1S_0$ metastable level of Ne^{++} (Daw, 2000). In this method, a decay curve is defined as $I'(t) = I(t)/Q(t)$, where $Q(t) = N(t)/N(0)$ and $N(t)$ is the number of ions stored in the trap. $I(t)$ denotes the observed photon signal rate. That is, a decay curve is the photon signal divided by the relative number of ions, as shown in Fig. 3. A detailed consideration of all populations and processes in the trap yields a function that can be fit to the decay curves to determine fundamental parameters for the rates of the processes, as discussed below. Basically, there are two decay components in the data: a fast decay component, due to decaying metastable ions, and a slow decay component, due to excited N_2^+ produced as a result of N_2^{++}+N_2 collisions. Thus, the data is well-described by the sum of two exponential decays.

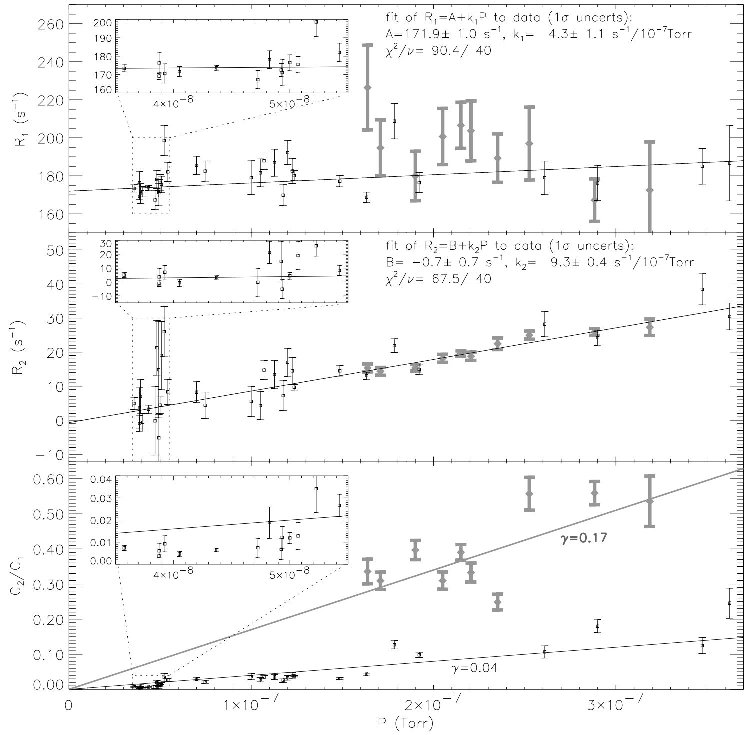

Fig. 4. Decay curves were collected for N_2 pressures ranging between 3×10^{-8} and 4×10^{-7} torr. The simplified form of $I'(t)$ (equation 6) was fit to the decay curves, yielding values for R_1 and R_2 *vs.* pressure, and values for the ratio C_2/C_1, which is a function of the photon detection bandpass, fill period, and pressure. The data above was collected using two different interference filters: one with a 11 nm FWHM bandpass centered at 213 nm (*black data*), and one with a 20 nm FWHM bandpass centered at 220 nm (*thick grey data*). Both transmittances are shown in Fig. 2. Linear fits to R_1 and R_2 as a function of P yielded results for: the radiative lifetime τ of $^5S_2$ N^+, the rate coefficient k_1, the dissociation rate B of N_2^{++}, and the rate coefficient k_2'.

The photon signal includes two sources of photons: radiative decay of metastable $^5S_2$ N^+, and collisions of ${N_2}^{++}$ with N_2.

$$I(t) = I_1(t) + I_2(t) \tag{1}$$

The signal rate for radiative decay photons is given by

$$I_1(t) = \epsilon_1 A N_1(t), \tag{2}$$

where ϵ_1 is the detection efficiency for the radiative decay photons, A is the total decay rate (or sum of A-values) for the radiative transitions being observed, and $N_1(t)$ is the number of metastable ions.

The signal rate for the collisionally-produced photons is given by

$$I_2(t) = \epsilon_2 k_2 P N_2(t), \tag{3}$$

where ϵ_2 is the probability (per collision) of detecting a photon, k_2 is the rate coefficient for the reaction $N_2 + N_2^{++} \rightarrow N_2^+ + N_2^+$, P is the N_2 pressure (converted to particle density for room temperature gas if k has units of cm^3/s), and $N_2(t)$ is the number of N_2^{++} ions. In detail, ϵ_2 is the probability distribution (in wavelength) for the photons generated by the collisions convolved with the bandpass of the photon detection system. This reaction has an exoergicity of 11.5 eV for ground-state reactants and products, and can easily produce two photons at wavelengths near 214 nm if both product ions are excited.

Because N^+ and ${N_2}^{++}$ have the same charge-to-mass ratio, the relative number of ions measured as a function of time reflects the combined population (both species). The functional form for the decay curve is obtained for this situation from a detailed consideration of rates for all collisional and non-collisional processes by solving the differential equations describing the level populations of both species.

Defining the following symbols:

$\tau =$ the radiative lifetime of $^5S_2$ N^+ (the reciprocal of the sum of the A-values for the 214 nm doublet)

$B =$ the dissociation rate of N_2^{++}

$k_0 =$ the rate coefficient for loss of N^+ ions via collisions with N_2

$k_1 =$ the difference between the ion-neutral collisional loss rate coefficient for the metastable level and the weighted average for the total ion population, plus the sum of rate coefficients for collisional de-excitation of the metastable level

$k_2 =$ the rate coefficient for the reaction $N_2^{++} + N_2 \rightarrow N_2^+ + N_2^+$

$k_3 =$ the ion-neutral collisional loss rate coefficient for N_2^{++} by all channels other than the reaction $N_2^{++} + N_2 \rightarrow N_2^+ + N_2^+$

$k_4 =$ the rate coefficient for creation of N^+ from N_2^{++} + N_2 collisions

$P =$ N_2 pressure (for k's with units of s^{-1}/torr), or particle density (for cm^3/s),

the fraction of N_2^{++} ions in the total ion population is given by

$$f(t) = [(f_0^{-1} - \delta)e^{R_2 t} + \delta]^{-1}, \tag{4}$$

where $R_2 = B + k_2' P$, $k_2' = k_2 + k_3 - k_0$, $\delta = (k_2' P - k_4 P - B)/R_2$, and $f_0 \equiv f(0)$. Note that the processes described by k_3 and k_4 are expected to not be significant, but in the final analysis, the impact of all processes on the measured parameters will be evaluated (including some processes omitted here for the sake of clarity). A full derivation is beyond the scope of this article, but a similar derivation may be found in Daw (2000). Here, the functional form for the decay curve is given by

$$I'(t) = C_1 e^{-R_1 t + R_2 t} f(t)/f_0 + C_2 f(t)/f_0 \tag{5}$$

where C_1 and C_2 are the detected photon rates at t=0 for the metastable decay and collisionally produced photons, and $R_1 = \tau^{-1} + k_1 P$.

For f_0=0.11, equation 5 for $I'(t)$ is very close in form to the sum of two exponentials:

$$I'(t) = C_1 e^{-R_1 t} + C_2 e^{-R_2 t} \tag{6}$$

with the decay rate R_1 pertaining to the metastable decay component of the decay curve, and the decay rate R_2 pertaining to the component produced by N_2^{++}+N_2 collisions.

Decay curves were collected for a number of N_2 pressures, and for the preliminary results, equation 6 was fit to the data to determine τ, k_1, B, and k_2' (see Fig. 4). For the final results, the complete form of $I'(t)$ will be fit to all decay curves simultaneously to determine additional parameters such as k_3 and k_4. Note that the rate coefficient k_0 for loss of N^+ via collisions with N_2 can be estimated from the measured loss rate of the (primarily N^+) ion signal, and since k_2' is much greater than k_3 and k_0, the rate coefficient for the reaction $N_2 + N_2^{++} \rightarrow N_2^+ + N_2^+$ can be determined by $k_2 = k_2' - k_3 + k_0$. Branching fractions into different excited states of N_2^+ will be determined by observing the corresponding emission bands of N_2^+. Finally, the production cross section for $^5S_2$ N^+ can be determined because the ratio of $^5S_2$ N^+ to N_2^{++} ions at t=0 is given by $(C_1/C_2)(\epsilon_2/\epsilon_1)(\tau k_2 P)$.

With this preliminary data, the result for the radiative lifetime of $^5S_2$ N^+ is 5.8 ± 0.1 ms, and the result for the dissociation rate of N_2^{++} is less than 1 s^{-1}. The rate coefficients are not presented yet, as the ion gauge was not calibrated for this preliminary work. Nevertheless, the data demonstrates the viability of the measurement method. For future data collection, a calibrated ion gauge will be used, amongst other improvements to the apparatus, resulting in lower uncertainties. For instance, we expect to measure the $^5S_2$ N^+ lifetime with an uncertainty of less than 1%, to help clarify the still inconclusive situation regarding this well-studied lifetime. The other atomic and molecular parameters to be measured will provide valuable information for ionospheric processes that currently have order-of-magnitude uncertainty associated with them. The cross section for production of $^5S_2$ N^+ by electron impact on N_2 currently has a factor of four uncertainty, and our measurement will help resolve whether the primary excitation is by solar photons or by electrons.

3. Proton Measurements

We are currently measuring rate coefficients for proton collisions with H_2 and He for their importance to the coupling of proton and neutral flows in sunspots, and for their importance to star formation in the early universe. Collision energies between protons and molecules in the experiment are typically a few eV or less and are controlled by the RF potential. At these energies, H^+ + He collisions are elastic, as no excited states are accessible. For $H^+ + H_2$ collisions, the charge exchange reaction $H_2 + H^+ \rightarrow H_2^+ + H$ has a threshold of 1.83 eV and both inelastic and elastic collisions occur. Since molecular hydrogen is observed in sunspots (Schüehle *et al.*, 1999) and starspots (Wood & Karovska, 2004), these collisional rates are important to the coupling of plasma and neutral flows.

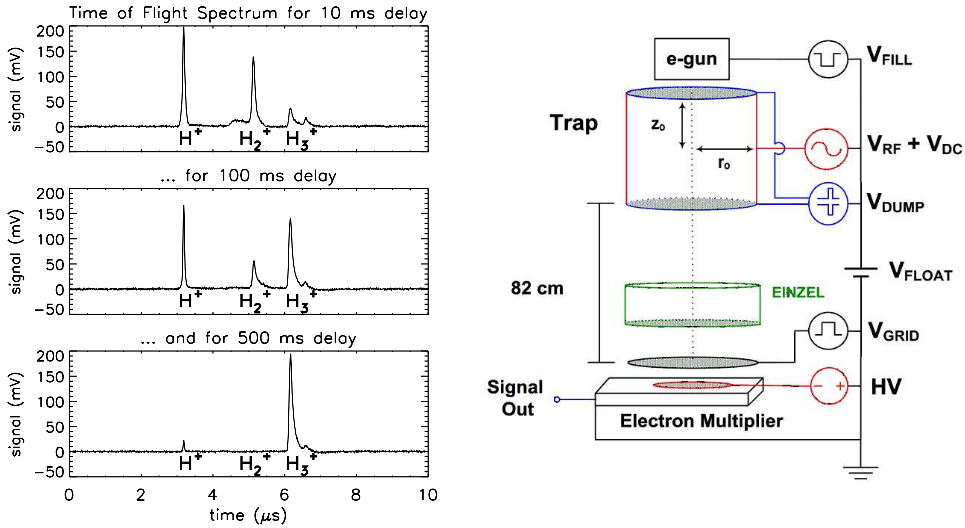

Fig. 5. *Left*: Time of flight spectra obtained when the trap was tuned to store H_2^+, shown for three different delay times after ions are created by electron impact. Note that the ion extraction was optimized for protons, so that protons arrive in a single peak, while the structure seen in the other ions' time of flight distributions provides valuable information on the ion temperatures in the trap. *Right:* A diagram of the apparatus and applied voltages. The trap dimensions are r_0=1.76 cm, z_0=1.86 cm.

The charge exchange process $H_2 + H^+ \rightarrow H_2^+ + H$ is predicted to be the dominant destruction mechanism of H_2 during the epoch of first star formation. However, the collision rate coefficient differs among published calculations by orders of magnitude (Savin *et al.*, 2004). Collision rate coefficients can be measured by observing the loss of the reactant(s) and or the growth of the product(s). In this case, the product H_2^+ reacts rapidly with H_2 to form H_3^+, as seen in Fig. 5. Also shown in this figure is the apparatus for the proton-hydrogen and proton-helium collision rate measurements, which is similar to that used for the nitrogen measurements, except that ion detection alone is sufficient for these measurements, and a longer flight path is used to obtain better charge-to-mass resolution. The reaction $H_2^+ + H_2 \rightarrow H_3^+ +$ H is being studied for its importance to ionospheric chemistry, and for its effect on the H_2^+ ions produced by $H_2 + H^+$ collisions in the ion trap. In the future, similar such reactions between ions and molecules can be studied.

4. Results and Discussion

The results from the preliminary nitrogen data collection are: 5.8 ± 0.1 ms for the radiative lifetime of $^5S_2$ N^+, and less than 1 s^{-1} for the dissociation rate of N_2^{++}. Further data collection will provide lower uncertainties for these parameters, and measurements of additional parameters such as the cross section for production of $^5S_2$ N^+ by electron impact on N_2, which will help to resolve whether the primary ionospheric excitation of N II] is by solar photons or electrons, and collision rate coefficients for H^++H_2 and H^++He collisions important to coupling of plasma and neutral flows in sunspots. A number of additional measurements are in progress, and researchers are encouraged to request and/or collaborate on the measurement of parameters relevant to their work.

Acknowledgements. We would like to thank all members of the local and scientific organizing committees for providing this invaluable opportunity to share scientific ideas, initiate collaborations, and conduct observations of the eclipse. We would like to thank Harvard University and the Smithsonian Astrophysical Observatory for resources toward initial exploration of the nitrogen work, and in particular, Alex Dalgarno, William H. Parkinson, and Peter L. Smith for informative discussions. Dr. Daw would like to thank the University of Hawaii IfA eclipse group, the many at Appalachian State University who supported this opportunity to collaborate on eclipse observations with the IfA group, and the people of Libya for their welcoming hospitality, support, and blessings of these scientific enterprises. The work on hydrogen is supported by NSF grant AST-04-06706 to Appalachian State University, NASA grant NAG5-5420 to Columbia University, and NSF grant AST-03-07203 to Columbia University. The work on nitrogen is supported by Research Corporation award CC6409 to Appalachian State University.

References

Bhatia, A. K., Kastner, S. O., and Behring, W. E.: 1982, *ApJ*, **257**, 887
Brage, T., Hibbert, A., and Leckrone, D.S.: 1997, *ApJ*, **478**, 423
Bucsela, E. J., Cleary, D. D., Dymond, K. F., and McCoy, R. P.: 1998, *J. Geophys. Res-Space Phys*, **103**, 29215
Bucsela, E. J. and Sharp, W. E.: 1989, *J. Geophys. Res*, **94**, 12069
Cleary, D. D. and Barth, C. A.: 1987, *J. Geophys. Res*, **92**, 13635
Cox S. G., Critchley A. D. J. , Kreynin P. S. , McNab I. R. , Shiell R. C., and Smith F. E.: 2003, *Phys. Chem. Chem. Phys.*, **5**, 663
Dalgarno, A., Victor, G. A., and Hartquist, T. W.: 1981, *Geophys. Res. Lett.*, **8**, 603
Daw A.: 2000, *Ph. D. thesis*, Harvard University
Daw A., Parkinson W. H., Smith P. L., and Calamai A. G.: 2000, *ApJ*, **533**, L179‘
Del Zanna, G., Landini, M., and Mason, H. E.: 2002, *A&A*, **385**, 968
Erdman, P.W., and Zipf, E.C.: 1986, *J. Geophys. Res-Space Phys.*, **91**, 1345
Halas, St., and Adamczyk, B.: 1972, *Int. J. Mass Spectrom. Ion Phys.*, **10**, 157
Hudson, C. E. and Bell. K. L.: 2005, *A&A*, **430**, 725
Lilensten J., Witasse O., Simon C., Solidi-Lose H., Dutuit O., Thissen R., and Alcaraz C.: 2005, *Geophys. Res. Lett.*, **32**, L03203
Mason, H. E., and Monsignori Fossi, B. C.: 1994, *A&A Rev.*, **6**, 123
Mathur, D.: 2004, *Phys. Rep.*, **391**, 1
Meier, R. R.: 1991, *Space Sci.Rev.*, **58**, 1
Mendoza, C., Zeippen, C. J., and Storey, P. J.: 1999, *A&AS*, **135**, 9
Price, S. P.: 2003, *Phys. Chem. Chem. Phys.*, **5**, 1717
Savin, D. W., Krstic, P. S., Haiman, Z. N., and Stancil, P. C.: 2004, *ApJ*, **607**, L147
Schüehle, U., Brown, C. M., Curdt, W., and Feldman, U.: 1999, in J. C. Vial, and B. Kaldeich-Schümann (Eds.), ESA SP-446: Proceedings of the 8th SOHO Workshop
Siskind, D. E. and Barth, C. A.: 1987, *Geophys. Res. Lett.*, **14**, 479
Tachiev, G., and Froese Fischer, C.: 2001, *Can. J. Phys.*, **79**, 955
Träbert, E., Wolf, A., Pinnington, E. H., Linkemann, J., Knystautas, E. J., Curtis, A., Bhattacharya, N., and Berry, H. G.: 1998, *Phys.Rev.A*, **58**, 4449
Vernazza, J. E. and Reeves, E. M.: 1978, *ApJS*, **37**, 485
Victor, G. A. and Dalgarno, A.: 1982, *Geophys. Res. Lett.*, **9**, 866
Wood, B. E. and Karovska, M.: 2004, *ApJ*, **60**, 502